FPD: Fringe Photometric Deflectometry When Fringe Meets Photometric Stereo

Ling Cao
Department of R&D
OPT Machine Vision
Dong Guan, China
caoling@optmv.com

Teng Wang
School of Mechatronic Engineering
Guangdong Polytechnic Normal University
Guang Zhou, China
Department of R&D
OPT Machine Vision
Dong Guan, China
wangteng@gpnu.edu.cn

Yong Yang
School of Mechatronic Engineering
Guangdong Polytechnic Normal University
Guang Zhou, China
yy2008@gpnu.edu.cn

Quan Tang
Department of R&D
OPT Machine Vision
Dong Guan, China
tangquan@optmv.com

Zi Meng Wang
Department of R&D
OPT Machine Vision
Dong Guan, China
wangzimeng@optmv.com

Wei Pan*
Department of R&D
OPT Machine Vision
Dong Guan, China
vpan@foxmail.com
*Corresponding author

***Abstract*—We present *Fringe Photometric Deflectometry* (FPD), a novel approach that synergistically combines Phase Measuring Deflectometry (PMD) and Photometric Stereo (PS) to achieve high-precision, full-field 3D surface reconstruction across both specular and diffuse regions. Leveraging PMD's accurate phase measurement for shiny surfaces and PS's detailed normal estimation for matte areas, we introduce an adaptive fusion mechanism that weights each modality according to local surface reflectance. We provide a rigorous theoretical formulation of the fusion process and validate its robustness through experiments on industrial test specimens. Our results demonstrate that FPD surpasses standalone PMD and PS in reconstruction accuracy and enhances defect detection capabilities, effectively revealing scratches, smudges, and other fine surface anomalies. FPD has been integrated into commercial inspection software, showcasing its practical utility.**

***Index Terms*—Phase Measuring Deflectometry, Photometric Stereo, 3D Reconstruction, Image Fusion, Surface Inspection**

I. Introduction

Accurate 3D surface reconstruction is essential for industrial inspection [1], cultural heritage preservation [2], and advanced manufacturing. Traditional techniques, such as Photometric Stereo (PS) [3] and Phase Measuring Deflectometry (PMD) [4] , excel under specific reflectance conditions but face limitations when applied to surfaces exhibiting both diffuse and specular components.

PS recovers surface normals by analyzing intensity variations under multiple illumination directions, performing well on Lambertian (diffuse) regions but degrading in presence of specular highlights [3], [5], [6]. Conversely, PMD captures surface gradients via structured fringe projection, yielding submicron accuracy on specular surfaces but providing unreliable data on matte areas [4], [7], [8].

In practical industrial applications, such as smartphone manufacturing or optical component inspection, accurate surface defect detection is critical. Existing methods often fail to detect subtle defects when specular highlights or diffuse textures dominate. By leveraging the complementary strengths of PMD and PS, FPD provides high-fidelity reconstructions that enhance defect visibility and localization. Our method has been integrated into commercial defect inspection software, demonstrating its real-world applicability and effectiveness in detecting both scratches and fingerprint smudges.

This paper introduces *Fringe Photometric Deflectometry* (FPD), an integrated framework that adaptively fuses PMD phase gradients and PS normal maps based on local reflectance properties. By dynamically weighting each modality according to computed glossiness measures, FPD achieves robust, high-fidelity reconstruction across complex surfaces. We summarize our key contributions:

- We propose FPD, a unified system that leverages the complementary strengths of PMD and PS for comprehensive surface analysis.
- We develop an adaptive fusion strategy that automatically balances PMD and PS contributions using per-pixel reflectance metrics.
- We present theoretical and empirical evidence demonstrating FPD's superiority over standalone methods in both reconstruction accuracy and defect detection.
- We integrate FPD into a commercial defect inspection pipeline, validating its practical effectiveness in real-world industrial scenarios.

The remainder of this paper is organized as follows: Sec-

tion II reviews related work; Section III details the FPD methodology; Section IV presents experimental validation; and Section V concludes and outlines future directions.

II. Related Work

A. Photometric Stereo

Photometric Stereo estimates surface normals from multiple images under varying lighting [3]. While calibrated PS assumes known light directions, uncalibrated PS methods use learning-based approaches for robustness [9]. PS struggles with specular reflections, leading to erroneous normal estimates [6]. Recent advances include robust outlier removal [10], spatially-varying BRDF modeling [11], and deep learning for specular handling [12].

B. Phase Measuring Deflectometry

PMD projects sinusoidal fringe patterns onto a scene and analyzes the reflected phase to compute surface slopes [4]. PMD excels on shiny surfaces but underperforms on diffuse regions due to low fringe contrast. Multi-frequency phase unwrapping [8] and single-shot deflectometry [13] have improved speed and reliability. Deep learning has also been applied to accelerate PMD processing and enhance the reconstruction accuracy [14].

C. Fusion of PS and PMD

Few works have attempted to merge PS and PMD data. Karami et al. [15] combined photogrammetry and PS for precise reconstruction. Shi *et al.* [16] proposed a weighted fusion of line-structured light and PS but faced challenges in highly reflective areas. To our knowledge, FPD is the first systematic integration of PS and PMD for unified surface reconstruction and defect detection.

D. Surface Defects Detection

For specular surface inspection, Cheng *et al.* [17] employed a dual-surface illumination model with PMD to accurately estimate surface gradients, enabling effective detection of scratches and coating bubbles. Bazeille *et al.* [18] proposed a dual-light linear scanning deflectometry method, achieving real-time 3D reconstruction and defect detection with 50-micron precision in industrial scenarios.

Fusion-based strategies further improve detection accuracy. Lan *et al.* [19] integrated surface normals, reflectance, and depth from photometric stereo to reconstruct fine-scale 3D topography for enhanced defect characterization. Wu *et al.* [20] introduced SIIA, which encodes multi-angle illumination into pseudo-color images via photometric stereo and deep learning, addressing challenges in lighting variation and complex geometry. Additionally, Qi *et al.* [21] proposed a dual-branch network to jointly extract geometric and photometric features from PMD phase data, significantly boosting detection on reflective surfaces.d modulation maps, significantly improving defect detection performance on reflective surfaces.

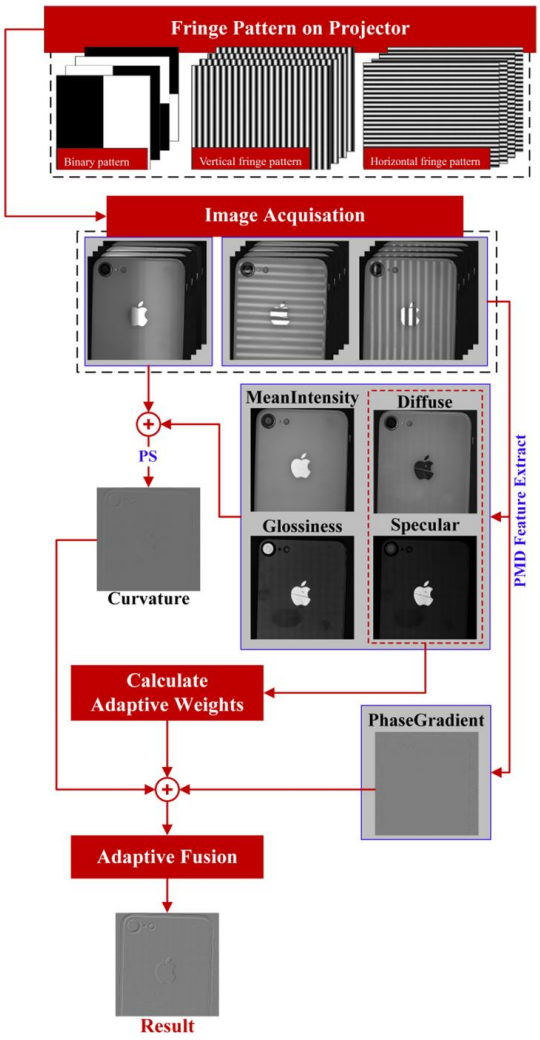

Fig. 1. Overview of the FPD framework, showing image acquisition, PS and PMD processing, and adaptive fusion stages.

III. Method

A. Overview

Fig. 1 illustrates the FPD pipeline. We capture three sets of fringe images: binary patterns for PS, and horizontal/vertical sinusoidal fringes for PMD. From these, we compute diffuse/specular components and glossiness measures, derive PS normal maps and PMD phase gradients, and perform adaptive fusion.

B. PMD Processing

The PMD pipeline is shown in Fig. 2. PMD projects sinusoidal fringes using an LCD screen. For each pixel (x, y) across N captured fringe images, the intensity can be modeled as:

$$I_n(x,y) = A(x,y) + B(x,y)\cos[\phi(x,y) + \delta_n] \quad (1)$$

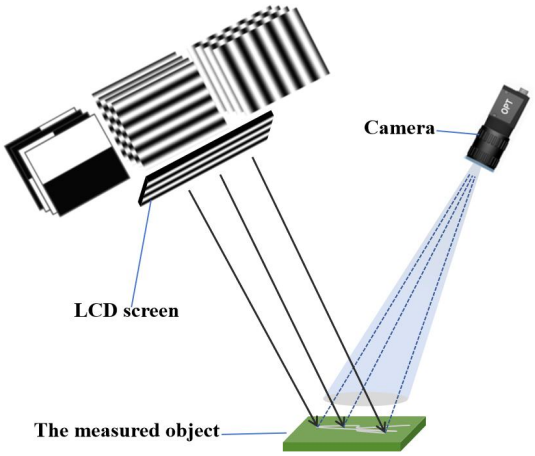

Fig. 2. A sketch of the FPD system setup(As reflection mode).

where $A(x, y)$ and $B(x, y)$ are the average and modulated intensities, respectively, and $\phi(x, y)$ is the wrapped phase. The phase shift δ_n is given by:

$$\delta\_n = \frac{2\pi n}{N}, \quad n = 1, 2, ..., N \tag{2}$$

With acquired images of intensity $I_n(x, y)$ (n=1,2,3,4), we can use a four-step phase-shifting approach to calculate the average intensity $A(x, y)$ as:

$$A(x, y) = \frac{1}{4} \sum_{n=1}^{4} I_n(x, y) \tag{3}$$

The specular component $S(x, y)$ and diffuse component $D(x, y)$ are computed as:

$$S(x, y) = \frac{\sqrt{\left(I_4 - I_2\right)^2 + \left(I_3 - I_1\right)^2}}{4A(x, y)} \tag{4}$$

$$D(x, y) = A(x, y) - S(x, y) \tag{5}$$

Glossiness is defined by:

$$O(x, y) = \frac{S(x, y)}{A(x, y)} \tag{6}$$

Multi-frequency unwrapping yields the absolute phase $\Phi(x, y)$:

$$\Phi(x, y) = \arctan\left(\frac{I_4 - I_2}{I_1 - I_3}\right) \tag{7}$$

The surface gradients can be calculated as:

$$G_x(x, y) = \frac{\partial \Phi_x}{\partial x}, \quad G_y(x, y) = \frac{\partial \Phi_y}{\partial y} \tag{8}$$

The phase gradient magnitude is:

$$P(x, y) = \sqrt{G_x(x, y)^2 + G_y(x, y)^2} \tag{9}$$

C. PS Processing

From the PMD results, we obtain mean intensity $M(x, y)$, specular reflection $S(x, y)$, diffuse reflection $D(x, y)$, and glossiness $G(x, y)$ maps. These reflection components serve as priors for the PS process. Combined with the four binary pattern images captured by the cameras, we construct the intensity matrix $M(f, p)$, where f is the number of images and p is the number of pixels. This matrix is then decomposed via Singular Value Decomposition (SVD):

$$M = U\Sigma V^T \tag{10}$$

The top three singular vectors in V^T approximate the surface normal matrix. Let (n_x, n_y, n_z) denote the normal components at each pixel. The surface gradients in x and y directions are computed as:

$$p = -\frac{n_x}{n_z}, \quad q = -\frac{n_y}{n_z} \tag{11}$$

Using these gradients, we compute the mean curvature $H(x, y)$ of the surface as follows:

$$H = \frac{(1 + q^2)p_{xx} - 2pqp_{xy} + (1 + p^2)q_{yy}}{2(1 + p^2 + q^2)^{3/2}} \tag{12}$$

This curvature estimation is implemented using CUDA-accelerated computations to ensure real-time performance. These curvature estimates are then integrated into the fusion process described in the next section to refine surface reconstruction.

D. Fusion Rationale

To effectively integrate PS and PMD, our fusion framework addresses the complementary nature of the two modalities. Theoretically, the fusion can be formulated as a weighted optimization problem. Let $P(x, y)$ denote the PMD-derived phase gradient map and $H(x, y)$ the PS-derived curvature map. The fused surface $Z(x, y)$ is estimated by minimizing the following energy function:

$$E(Z) = \int \left[w_{PMD} \|\nabla Z - P\|^2 + w_{PS} \|\nabla Z - H\|^2 \right] dxdy \tag{13}$$

where w_{PMD} and w_{PS} are spatially adaptive weights reflecting confidence in PMD and PS measurements, respectively.

Specifically, our considerations include:

- Employing the adaptive weighting to balance the contributions of PS and PMD based on the local surface reflectance characteristics.
- Incorporating robust phase unwrapping techniques to minimize errors in PMD gradient estimation, especially in regions with surface discontinuities.
- Utilizing GPU-accelerated computation to manage the increased processing complexity introduced by dual-modality fusion.

In practice, since the PMD pipeline yields both specular and diffuse reflection components, we design an adaptive fusion

strategy that uses these components directly to compute the weights:

- **Weight Computation:** The weights w_{PMD} and w_{PS} are computed based on the relative strength of specular and diffuse components. For regions with high glossiness (i.e., $G(x, y) > \theta$), PMD receives higher confidence; for more diffuse regions, PS is prioritized.
- **Adaptive Weight Calculation:** To ensure smooth transitions between specular and diffuse areas, we define the weights as:

$$w_{PMD} = \frac{S(x, y)}{S(x, y) + D(x, y)}$$
$$w_{PS} = \frac{D(x, y)}{S(x, y) + D(x, y)} \tag{14}$$

- **Final Fusion:** The fused reconstruction result $R(x, y)$ is obtained by linearly combining the two modalities:

$$R(x, y) = w_{PMD} P(x, y) + w_{PS} H(x, y) \tag{15}$$

This adaptive strategy ensures that PMD dominates in highly specular regions—where fringe patterns are more reliable—while PS governs reconstruction in diffuse areas, preserving fine surface details. The combined result provides a balanced and accurate reconstruction across varying surface types.

IV. Experiments

A. Experimental Setup

To validate the effectiveness of the proposed method, we constructed an experimental platform, as shown in Fig. 3, which consists of a projector, a camera, and corresponding mounting structures. The experimental environment is based on a Windows 10 Professional operating system, equipped with an Intel Core i5-13500 CPU (2.50 GHz) and an NVIDIA GeForce RTX 3060 GPU (12 GB).

Our method targets non-Lambertian object surfaces exhibiting both diffuse and specular reflections. We selected the back surface of an iPhone as the test object, as it exhibits both types of reflection. During the experiment, a sequence of predesigned periodic fringe patterns was projected onto the surface of the object, including binary fringe patterns, horizontal fringe patterns (fringe-x), and vertical fringe patterns (fringe-y).

Binary patterns are employed to simulate four-quadrant illumination for photometric stereo (PS), while fringe-x and fringe-y patterns are used for phase-measuring deflectometry (PMD). The system captures a total of 12 fringe images per cycle, corresponding to the three types of patterns mentioned above.

B. Reconstruction Comparison

Using the described experimental setup, we performed surface reconstruction and evaluated its effectiveness in defect detection. Fig.4(a) shows the mean curvature map obtained from PS using binary illumination; Fig.4(c) presents the final result of our fused photometric deflectometry (FPD) method.

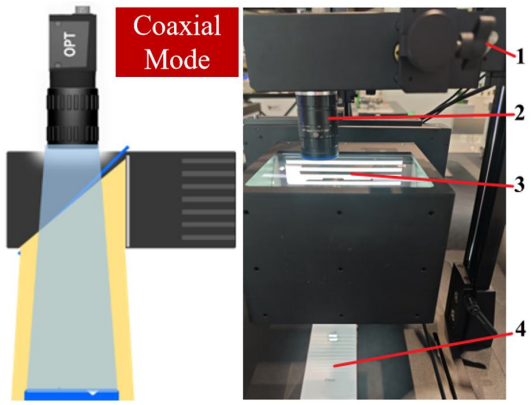

(a) (b)

(c)

Fig. 3. Experimental platform: (a) Schematic diagram of the system setup; (b) Overhead view of the specimen and hardware assembly(1. Corresponding mounting structure, 2. Camera, 3. Projector, 4. Measured object);(c) phone back plate to be inspected.

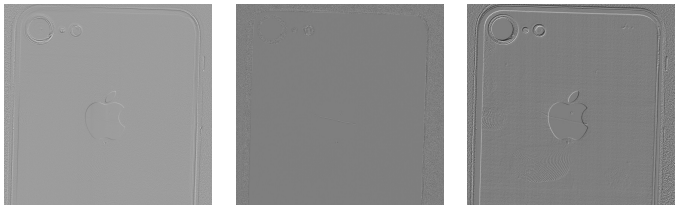

(a) (b) (c)

Fig. 4. Surface reconstruction results: (a) PS mean curvature map, (b) PMD phase gradient map, (c) FPD fusion result.

The results demonstrate that the PS-based mean curvature map fails to capture fine defects such as scratches in regions with strong specular reflections (e.g., the logo area). In contrast, the PMD-derived phase gradient map struggles to reconstruct smudges in areas with weaker specular components (e.g., regions outside the logo). Our proposed FPD method achieves superior performance across both types of features, yielding more complete and consistent reconstructions.

C. Defection Detect Analysis

To further validate the advantages of the proposed FPD method over individual techniques, we conducted defect detection experiments using “Smart3,” a commercial software

developed by OPT Machine Vision. Detection was performed on the three types of reconstructed results in Fig.4, focusing on surface scratch detection (Fig.5) and fingerprint/smudge detection (Fig. 6).

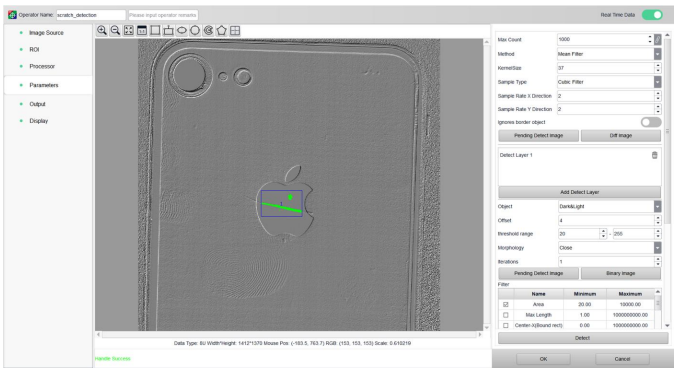

Fig. 5. Smart3 interface: scratch detection operation.

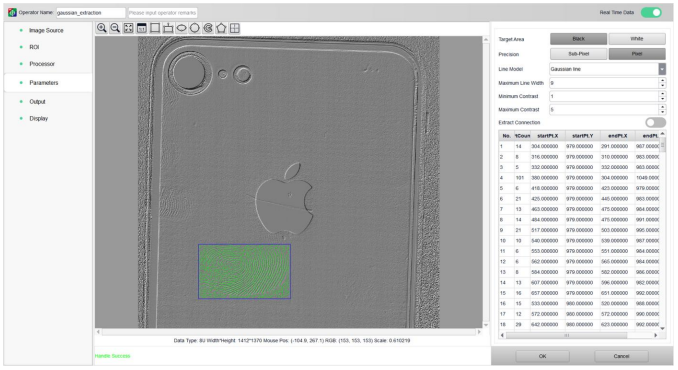

Fig. 6. Smart3 interface: fingerprint/smudge detection via Gaussian line extraction.

The detection outcomes are shown in Fig.7. PS-based reconstruction fails to detect features in regions with strong specular reflections (Fig.7(a)), while PMD fails in areas with weaker reflections (Fig.7(b)). In contrast, the FPD result (Fig.7(c)) effectively supports both types of defect detection.

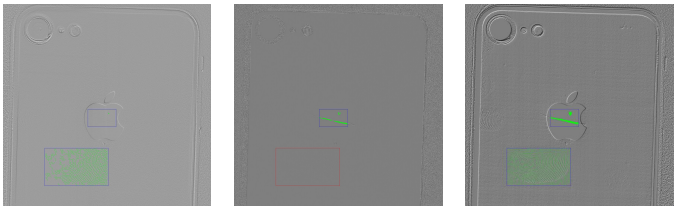

(a) (b) (c)

Fig. 7. Defect detection results: (a) PS-based detection, (b) PMD-based detection, (c) FPD-based detection with improved performance.

These experiments confirm that FPD provides a more robust and comprehensive representation of surface details, enabling reliable detection of fine defects under varying reflectance conditions.

V. Conclusion and Future Work

The proposed FPD framework, integrating photometric stereo and phase-measuring deflectometry, demonstrates enhanced surface reconstruction performance for non-Lambertian objects. Experimental results show that FPD outperforms standalone PS and PMD methods in reconstructing and detecting surface scratches and smudges, particularly under challenging reflective conditions. These advantages highlight the potential of FPD for industrial surface inspection and quality control applications, where high precision and robustness are required. Future work will focus on the calibration processs of the integrated system and develop height measurement for complex surfaces.

VI. Acknowledgment

This research is fully conducted and supported by OPT Machine Vision.

References

[1] Y. Ju, M. Jian, C. Wang *et al.*, "Estimating high-resolution surface normals via low-resolution photometric stereo images," *IEEE Transactions on Circuits and Systems for Video Technology*, vol. 34, no. 4, pp. 2512–2524, 2023.

[2] F. Gao, Y. Xu, and X. Jiang, "Near optical coaxial phase measuring deflectometry for measuring structured specular surfaces," *Optics Express*, vol. 30, no. 10, pp. 17 554–17 566, 2022.

[3] R. i. Woodham, "Photometric method for determining surface orientation from multiple images," *Optical Engineering*, vol. 19, no. 1, pp. 139–144, 1980.

[4] Y. Xu, F. Gao, and X. Jiang, "A brief review of the technological advancements of phase measuring deflectometry," *PhotoniX*, vol. 1, no. 1, p. 14, 2020.

[5] L. Abada and S. Aouat, "Improved photometric stereo based on local search," *Multimedia Tools and Applications*, vol. 81, no. 21, pp. 31 181–31 195, 2022.

[6] S. Tozza, R. Mecca, M. Duocastella, and A. Del Bue, "Direct differential photometric stereo shape recovery of diffuse and specular surfaces," *Journal of Mathematical Imaging and Vision*, vol. 56, pp. 57–76, 2016.

[7] Z. Zhang, Y. Wang, F. Gao *et al.*, "Enhancement of measurement accuracy of discontinuous specular objects with stereo vision deflectometer," *Measurement*, vol. 188, p. 110570, 2022.

[8] Y. Xie, X. Wang, and Q. Zhou, "Phase calculation of smooth surface with multi-reflectivity based on phase measurement deflectometry," *Optics Express*, vol. 32, no. 12, pp. 20 866–20 880, 2024.

[9] Z. Li, Z. Lu, H. Yan *et al.*, "Spin-up: Spin light for natural light uncalibrated photometric stereo," *Proceedings of the IEEE/CVF Conference on Computer Vision and Pattern Recognition*, 2024.

[10] T.-P. Wu and C.-K. Tang, "Photometric stereo via expectation maximization," *IEEE Transactions on Pattern Analysis and Machine Intelligence*, vol. 32, no. 3, pp. 546–560, 2009.

[11] D. Goldman, B. Curless, A. Hertzmann, and S. Seitz, "Shape and spatially-varying brdfs from photometric stereo," *IEEE Transactions on Pattern Analysis and Machine Intelligence*, vol. 32, no. 6, pp. 1060–1071, 2009.

[12] R. Yang, Y. Wang, S. Liao, and P. Guo, "Dpps: A deep-learning based point-light photometric stereo method for 3d reconstruction of metallic surfaces," *Measurement*, vol. 210, p. 112543, 2023.

[13] M. Nguyen, Y.-S. Ghim, and H.-G. Rhee, "One-shot deflectometry for high-speed inline inspection of specular quasi-plane surfaces," *Optics and Lasers in Engineering*, vol. 147, p. 106728, 2021.

[14] L. Fan, Z. Wu, J. Wang *et al.*, "Deep learning-based phase measuring deflectometry for single-shot 3d shape measurement and defect detection of specular objects," *Optics Express*, vol. 30, no. 15, pp. 26 504–26 518, 2022.

[15] A. Karami, F. Menna, and F. Remondino, "Combining photogrammetry and photometric stereo to achieve precise and complete 3d reconstruction," *Sensors*, vol. 22, no. 21, p. 8172, 2022.

[16] J. Shi, Y. Li, Z. Zhang, T. Li, and J. Zhou, "Adaptive weighted data fusion for line structured light and photometric stereo measurement system," *Sensors*, vol. 24, no. 13, p. 4187, 2024.

[17] X.-M. Cheng, T.-T. Wang, W.-B. Zhu, B.-D. Shi, and W. Chen, "Phase deflectometry for defect detection of high reflection objects," *Sensors*, vol. 23, no. 3, p. 1607, 2023.

[18] S. Bazeille, A. Meguenani, K. Tout, S. Kohler, O. Jrad, J.-P. Chambard, and C. Cudel, "A scanning deflectometry scheme for online defect detection and 3-d reconstruction of specular reflective materials," *The International Journal of Advanced Manufacturing Technology*, vol. 131, no. 1, pp. 245–259, 2024.

[19] J. Lan and J. Shi, "Photometric stereo multi-information fusion unsupervised anomaly detection algorithm," *Applied Optics*, vol. 63, no. 24, p. 6345, aug 2024. [Online]. Available: https://opg.optica.org/ao/abstract.cfm?doi=10.1364/AO.524199

[20] L. Wu, Y. Ran, L. Yan, Y. Liu, Y. Song, and D. Han, "A dataset for surface defect detection on complex structured parts based on photometric stereo," *Scientific Data*, vol. 12, no. 1, pp. 1–16, 2025.

[21] Z. Qi, Z. Wang, J. Huang, Q. Duan, C. Xing, and J. Gao, "Phase-modulation combined deflectometry for small defect detection," *Applied Optics*, vol. 59, no. 7, pp. 2016–2023, 2020.